

**Closed-orbit recurrences in molecular hydrogen**J. D. Wright,<sup>\*</sup> J. M. DiSciaccia,<sup>†</sup> J. M. Lambert,<sup>‡</sup> and T. J. Morgan*Department of Physics, Wesleyan University, Middletown, Connecticut 06459, USA*

(Received 30 January 2010; published 9 June 2010)

Using scaled-energy Stark spectroscopy, we report the observation of recurrences due to closed orbits, both geometric and diffractive, in the  $\nu = 0$ ,  $R = 1$ ,  $nd$  Rydberg series of  $H_2$  ( $16 < n < 26$ ) interacting with the  $\nu = 0$ ,  $R = 3$  series ( $13 < n < 15$ ). The data support the molecular closed-orbit theory prediction of diffractive trajectories due to inelastic scattering of the excited electron on the molecular core. We have made similar measurements in He, and a comparison between the recurrence properties of  $H_2$  and its united atom equivalent is given.

DOI: [10.1103/PhysRevA.81.063409](https://doi.org/10.1103/PhysRevA.81.063409)

PACS number(s): 32.80.Ee, 33.15.-e, 33.80.-b, 32.60.+i

**I. INTRODUCTION**

In 1988 Eichmann *et al.* [1] launched the experimental technique of scaled-energy recurrence spectroscopy (SERS) as a method to reveal and study semiclassical dynamics in complex experimental spectra. The method received significant impetus with the development of closed orbit theory (COT) for atomic hydrogen by Du and Delos [2]. The theoretical basis for the advancement of COT, which describes atomic dynamics utilizing the concepts of trajectory and orbits, occurred earlier with the full development of periodic orbit theory by Gutzwiller in 1971 [3]. During the last decade COT has been modified and applied to nonhydrogenic atoms [4–7] resulting in very good agreement with many Stark SERS experimental studies including those in sodium [1,8], lithium [9,10], barium [11–13], calcium [13], helium [14–18], argon [19,20], and strontium [21]. This is also true for other experiments employing SERS with magnetic fields [22–24]. Considering the substantial success of COT in atoms, it is not surprising that recently the semiclassical theory has been extended to molecules (MCOT), by merging COT with molecular quantum defect theory [25–27].

In this article we report the results of an experimental investigation that extends SERS to molecules. Using scaled-energy Stark spectroscopy we investigate directly the effects of a molecular core on the recurrence spectrum. In particular, we observe molecular-hydrogen recurrences that reveal the interaction between the electronic and nuclear motion via inelastic diffractive trajectories as predicted by MCOT [25,26]. Specifically, we observe a region of the photoexcitation spectrum of  $H_2$ , partially observed originally in zero-field by Kachru and Helm [28], in which the  $\nu = 0$ ,  $R = 1$ ,  $nd$  Rydberg series ( $16 < n < 26$ ) overlaps the  $\nu = 0$ ,  $R = 3$  series ( $13 < n < 15$ ), as shown in Fig. 1. These states lie below the  $R = 0$  ionization continuum and converge to series limits associated with rotationally excited states of the  $H_2^+$  core. (We use atomic units and  $\nu$ ,  $N$ , and  $R$  as the quantum numbers for vibration, initial-state rotation, and final-state rotation.) The states are accessed by laser excitation of the  $\nu = 0$ ,  $N = 1$ ,  $1s\sigma^2 p\pi c^3 \Pi_u^-$  metastable state. The excitation process is the same as that in [28] and is known to populate predominantly

the  $nd$  Rydberg series of ortho-hydrogen. The excited states are detected by field ionization. The relatively simple structure of the  $H_2$  molecule in this region, which still includes core dynamics due to multichannel effects, makes it particularly attractive to semiclassical analysis.

**II. DISCUSSION**

It is well known for atomic hydrogen that the classical Stark Hamiltonian is not dependent on the binding energy of the electron and the electric field separately, but rather on scaled energy only. Scaled-energy spectroscopy measures the experimental photoabsorption spectrum at a constant scaled energy  $\epsilon = EF^{-1/2}$  over a range of  $n$ , where  $F$  is the applied electric field and  $E$  is the electron binding energy relative to the Rydberg series limit. Experimentally, to maintain the scaled energy fixed, the laser wavelength and the electric field are adjusted accordingly, while recording data. Recording data at fixed scaled energy holds the Hamiltonian constant and maintains the same classical dynamics over the entire range of the measured spectrum. This allows a dynamical interpretation of the spectrum via an appropriate Fourier transformation that gives peaks at scaled actions  $S$  of the classical closed orbits of the system, known as the scaled-energy recurrence spectrum. In a similar fashion to our previous work on argon, [20] we carry out the Fourier transformation with respect to the effective principal quantum number  $n^* = (-2E)^{-1/2}$  where  $E = 0$  corresponds to  $n^* = \infty$  of the  $R = 1$  Rydberg series [29]. This approach yields a scaled-action coordinate that is independent of scaled energy and localizes the primitive recurrence peak of a scaled Rydberg series at action  $S = 1$ . The recurrence spectrum at low scaled action is much simpler than the photoabsorption spectrum and yields relatively few discrete peaks at scaled actions of closed orbits associated with electron motion that periodically closes at the core, as well as their repetitions and combinations created by scattering of the Rydberg electron off the core. An important result of MCOT is that not only elastic but also inelastic scattering must be considered in molecules, with the relative importance depending on the molecular quantum defects of the system [25,26]. For a real physical molecular system, the scaling law does not hold exactly due to the internal structure of the molecular ion core and this complicates detailed semiclassical analysis [30]. To circumvent this complication, a careful choice of the molecule and laser excitation scheme is necessary. Inspired by the successes and robustness of COT

<sup>\*</sup>Present address: Physics Dept., Yale University.<sup>†</sup>Present address: Physics Dept., Harvard University.<sup>‡</sup>Present address: Physics Dept., Fieldston School.

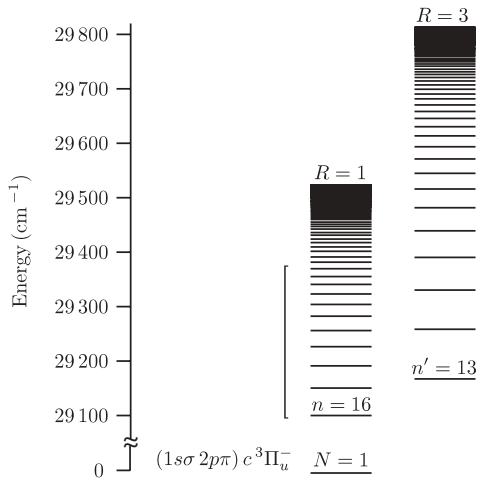


FIG. 1. Energy level diagram of  $\text{H}_2$ ,  $R = 1$ , and  $R = 3$   $nd$  Rydberg triplet states. The bracketed region shows the measured laser-energy range of the present experiment. It contains three levels of the  $R = 3$  series embedded in the  $R = 1$  series, which results in variations in oscillator strength, peak position, and quantum defects. One additional rotational line is also present due to the  $R = 5$  series (not shown).

and SERS, including complex multichannel atoms (which do not scale exactly), we perform SERS measurements of  $\text{H}_2$  relative to the  $R = 1$  series and consider the dynamics from the standpoint of the  $R = 1$  core configuration, knowing full well that the embedded  $R = 3$  rotational series scales only approximately. We are able to show that certain features in the recurrence spectrum of molecular hydrogen can be associated with different dynamical regimes of the Rydberg electron and can be understood in terms of inelastic scattering predictions from MCOT. Additionally, we make use of a complimentary approach introduced by Jensen *et al.* [16] to qualitatively explain certain features in the recurrence spectrum that correspond with the quantum mechanical Stark structure, and we show that low scaled-action features in the recurrence spectrum are manifestations of certain regularities present in the experimental spectrum.

### III. EXPERIMENT

The apparatus used in the present work is similar to that used and described in previous publications and we refer the reader to these papers for more detail [19,20]. A 4 keV  $\text{H}_2^+$  ion beam from a Colutron filament ion source is passed through a cell containing potassium vapor. A fraction of the beam ( $\sim 15\%$ ) is neutralized via electron transfer collisions in the cell, with a large fraction ( $\sim 80\%$ ) of the neutrals in the  $1s\sigma 2p\pi c^3\Pi_u^-$  metastable state. Unneutralized ions are removed from the beam by an electric field and monitored. The  $\text{H}_2$  beam, with a typical effective current in the range of 50 to 100 nanoamps, traverses 39 cm (pressure  $\sim 10^{-7}$  Torr) through a pair of parallel plates to which a voltage is applied to provide a constant electric field perpendicular to the  $\text{H}_2$  beam. A laser beam, propagating counter collinearly, overlaps the neutral beam and excites molecules to Rydberg states in the presence of the electric field. The laser beam is produced by an Nd:YAG laser (20 Hz) that pumps a tunable dye

laser (20 mJ at 480 nm) the output of which is frequency doubled using a potassium titanyl phosphate (KTP) crystal with an efficiency of  $\sim 15\%$ . Linearly polarized light was oriented parallel to the electric field exciting  $M = 0$  states. Immediately after the parallel plates, the beam passes through a field ionizer consisting of two parallel plates separated by 1 mm with 1 mm holes and oriented to produce an electric field of about 8 kV/cm longitudinal to the beam. This field ionizes Rydberg molecules down to the principal quantum number  $n \sim 16$  ( $n^4 F = 6 \times 10^8$ ) and accelerates the resulting ions into an electrostatic analyzer followed by a channel plate detector. The modulated  $\text{H}_2^+$  signal from field ionization is amplified and recorded.

### IV. RESULTS

We present data for scaled energies  $\varepsilon = -2.3$  and  $-3.2$  [31]. These energies span two different dynamical regimes from the strong field region near the classical ionization limit ( $\varepsilon = -2.0$ ) where the Stark manifolds are well overlapped, to the weak field region just inside the Inglis-Teller limit ( $\varepsilon = [3n/4]^{1/2}$ ), where the Stark manifolds begin to overlap. Figure 2 shows experimental spectra from field ionization for molecular hydrogen at  $\varepsilon = -2.3$  and  $-3.2$  and for comparison helium at  $\varepsilon = -2.3$ .

These spectra account for the dynamical characteristics found in the recurrence spectra. The  $\text{H}_2$  and He spectra when compared at  $\varepsilon = -2.3$  [Figs. 2(a) and 2(c)] are visually very different. The  $\text{H}_2$  spectra are complex and close inspection of the data reveals a low-frequency modulation with a period of  $\delta n \sim 3$  that is not present in He. The Fourier transform of experimental spectra, the recurrence spectra, are shown in Fig. 3. The data for  $\text{H}_2$  and He were taken separated by several months using the same apparatus. Small differences in peak position between  $\text{H}_2$  and He arise from variations in the quantum defects and from the uncertainty in the scaled-energy measurements due to nonlinearity in the laser scanning, uncertainty in the electric field, and absolute energy calibration between the different measurements.

When two rotational series are present in the absorption spectrum, MCOT asserts that new peaks appear in the recurrence spectrum, due to the presence of the low  $n'$  series, at scaled actions less than that of the primitive recurrence peak of the high- $n$  main series. These peaks can be seen in Fig. 3 and are labeled  $p'$ . MCOT also predicts that when the two series interact, additional new peaks appear associated with rotationally inelastic core scattering that occurs when the semiclassical wave function of a geometric closed orbit returns to the core and diffracts (inelastically scatters) to produce a new outgoing trajectory whose properties are dependent on the laser excitation energy and the accessible core configurations [25,26]. These peaks which appear at combined scaled actions of primitive classical trajectories, for example  $S_p + S_{p'}$ , are labeled  $d$  in Fig. 3. The caption of Fig. 3 explains the peaks in the figure in more detail.

The interchannel mixing responsible for the inelastic scattering is represented in MCOT by the quantum scattering  $T$  matrix,  $T_\alpha = \exp(2i\pi\mu_\alpha) - 1$ , where  $\mu_\alpha$  is the quantum defect for the core configuration  $\alpha$  [25,26]. An inelastic scattered orbit is a combination of two different orbits at two

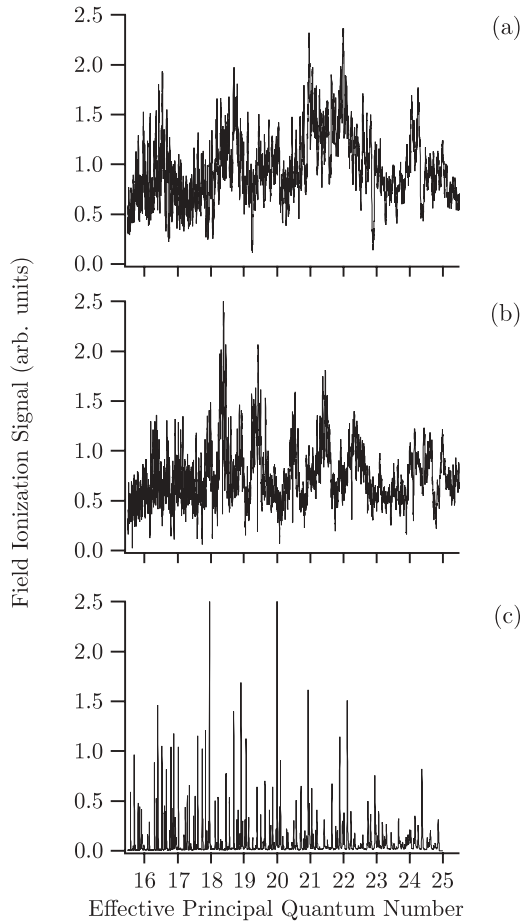


FIG. 2. Experimental spectrum of triplet,  $M = 0$   $\text{H}_2$  and He, obtained by laser excitation of  $1s\sigma\ 2p\pi\ c^3\Pi_u^-$  metastable  $\text{H}_2$  and  $1s\ 2s^3S_1$  metastable He, in the presence of an electric field and detected using field ionization. (a)  $\text{H}_2$  at  $\varepsilon = -2.3$ , (b)  $\text{H}_2$  at  $\varepsilon = -3.2$ , and (c) He at  $\varepsilon = -2.3$ .

different energies resulting from the exchange of electronic and rotational energies, a process not possible in atoms, and the recurrence peak associated with this process appears in the spectrum at the “diffractive” combination of their two scaled actions. As can be seen from the figure, the diffractive contributions to the recurrence spectrum are quite different for the two scaled energies shown, and confirm the importance of inelastic scattering in the recurrence spectra.

In Fig. 4, we show a simplified picture of the semiclassical photoabsorption process that gives rise to the new molecular peaks in the recurrence spectrum.

From a different point of view, MCOT predictions can be understood in a complementary quantum mechanical fashion by considering the regularities present in the experimental spectra. As was shown by Jensen *et al.* [16] for helium and by Wright *et al.* [20] for argon, additional periodicities in the scaled-energy photoabsorption spectrum arise due to level interactions not present in atomic hydrogen and create new structures in the recurrence spectrum that can be associated with core scattering [5,6,34]. In the present case, the interval in the experimental spectra between levels of the low- $n'$  series is much larger than the average spacing of states in the main, high- $n$ , Rydberg series and consequently the Fourier transform

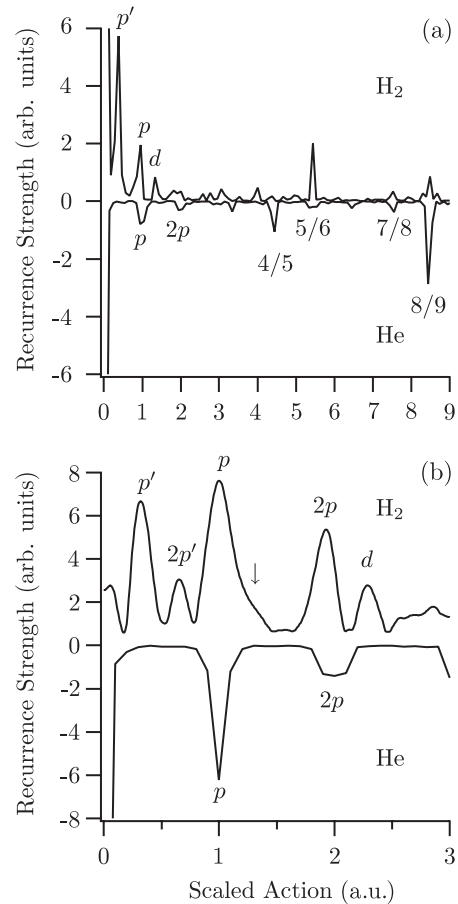


FIG. 3. Recurrence spectra of triplet,  $M = 0$   $\text{H}_2$  and He, obtained by Fourier transforming the experimental data. The spectra are normalized to have the same total recurrence strength. The He spectra are much simpler than those of  $\text{H}_2$ . (a) Spectrum at  $\varepsilon = -2.3$ . The classical bifurcation point is  $S = 3.8$ . In He, the two lowest scaled-action peaks are the primitive orbit recurrence  $p$  and its repetition  $2p$ . The peaks to the right of the bifurcation are created by classical closed orbits that are labeled by the period ratio of motion in the  $u$  and  $v$  semiparabolic coordinates. In  $\text{H}_2$ , the peaks labeled  $p'$  and  $p$  are the primitive recurrences of the  $R = 3$  and  $R = 1$  rotational series. The peak at the sum of these scaled actions,  $S = 0.39 + 0.94 = 1.33$ , is a diffractive inelastic-scattering recurrence, labeled  $d$  in the figure. The region between peak  $d$  and the bifurcation point contains repetitions and ghost orbits [32,33]. (b) Low scaled-action spectrum at  $\varepsilon = -3.2$ . The He spectrum shows a primitive peak and repetition. The  $\text{H}_2$  scan (background subtracted) shows the  $R = 1$  and  $R = 3$  primitive orbits (labeled  $p$  and  $p'$ ) and their first repetitions (labeled  $2p$  and  $2p'$ ). The strong peak at  $S = 2.27$  (labeled  $d$ ) results from diffractive inelastic scattering between the primitive  $R = 1$  orbit at  $S = 1.95$  ( $2p$ ) and the  $R = 3$  primitive orbit at  $S = 0.32$  ( $p'$ ). The shortest diffractive peak ( $p' + p$ ) is suppressed and shows only as a shoulder in the spectrum, identified by an arrow.

will produce a low  $n'$ -series primitive peak with scaled action less than 1, the smallest, scaled action of the regular, main series. This peak at  $S = 0.39$  can be seen in Fig. 3(a) and is labeled as  $p'$ . This peak does not correspond to a specific closed orbit since the  $N = 3$  series is unscaled, rather it is caused by a coherent superposition of primitive orbits related

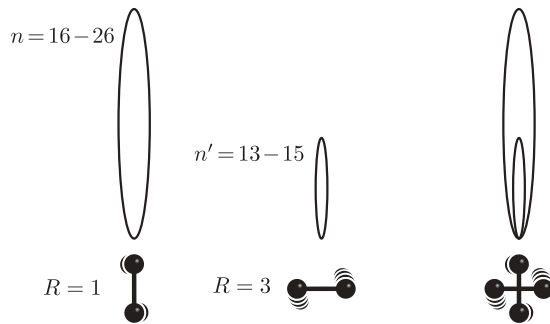


FIG. 4. Illustration of multichannel semiclassical dynamics between the Rydberg electron and nuclei in  $H_2$ . Far from the core, the Rydberg electron is uncoupled from the  $R = 1$  and  $R = 3$  freely rotating nuclei and executes a geometric trajectory. The Rydberg electron may scatter off the core and exchange energy with the core, resulting in a diffractive orbit that combines the two geometric orbits of the  $R = 1$  and  $R = 3$  core configurations.

to the scaled-energy range of the  $R = 3$  series that is accessed in the measurements.

To our knowledge, a direct comparison between the observed recurrences and predictions of MCOT is not available [35]. The recurrence spectrum of a molecule is very sensitive to the quantum defects associated with the projection of the electronic angular momentum onto the molecular axis since the dynamics are coupled to the rotating molecular axis

when the electron is near the core. In the present case, the initial state is the  $1s\sigma 2p\pi c^3\Pi_u^-$  metastable state, and there are three important quantum defects  $\mu_\Sigma = 0.071$ ,  $\mu_\Pi = 0.045$ , and  $\mu_\Delta = -0.017$  that play a role in determining the details of the peaks in the recurrence spectrum, along with two rotational configurations  $N = 1$  and  $3$  [36]. Also, since  $H_2$  is the lightest of all molecules, the value of the rotational constant is especially large ( $1.33 \times 10^{-4}$ ) resulting in a relatively large gap between the ionization limits of the different rotational channels and thereby introducing computational complications [26] as well as lower-energy states which may not have attained the semiclassical limit.

## V. CONCLUSION

We measured the recurrence spectra of  $H_2$  in an electric field and confirmed the generic predictions of molecular closed-orbit theory concerning the importance of rotationally inelastic scattering on the core. It should be possible to apply the present approach to other molecules and we are pursuing this direction.

## ACKNOWLEDGMENTS

We wish to acknowledge the NSF for support and Eric Sia for assistance in the laboratory.

- 
- [1] U. Eichmann, K. Richter, D. Wintgen, and W. Sandner, *Phys. Rev. Lett.* **61**, 2438 (1988).
- [2] M. L. Du and J. B. Delos, *Phys. Rev. A* **38**, 1896 (1988).
- [3] M. C. Gutzwiller, *J. Math. Phys.* **12**, 343 (1971).
- [4] T. S. Monteiro and G. Wunner, *Phys. Rev. Lett.* **65**, 1100 (1990).
- [5] D. Delande *et al.*, *J. Phys. B* **27**, 2771 (1994).
- [6] B. Hüpper, J. Main, and G. Wunner, *Phys. Rev. Lett.* **74**, 2650 (1995).
- [7] P. A. Dando, T. S. Monteiro, D. Delande, and K. T. Taylor, *Phys. Rev. Lett.* **74**, 1099 (1995).
- [8] S. N. Pisharody, J. G. Zeibel, and R. R. Jones, *Phys. Rev. A* **61**, 063405 (2000).
- [9] M. Courtney, H. Jiao, N. Spellmeyer, and D. Kleppner, *Phys. Rev. Lett.* **73**, 1340 (1994).
- [10] N. Spellmeyer, D. Kleppner, M. R. Haggerty, V. Kondratovich, J. B. Delos, and J. Gao, *Phys. Rev. Lett.* **79**, 1650 (1997).
- [11] G. J. Kuik *et al.*, *J. Phys. B* **29**, 2159 (1996).
- [12] K. A. Bates, J. Masae, C. Vasilescu, and D. Schumacher, *Phys. Rev. A* **64**, 033409 (2001).
- [13] J. Murray-Krezan, J. Kelly, M. R. Kutteruf, and R. R. Jones, *Phys. Rev. A* **75**, 013401 (2007).
- [14] M. Keeler and T. J. Morgan, *Phys. Rev. Lett.* **80**, 5726 (1998).
- [15] M. L. Keeler and T. J. Morgan, *Phys. Rev. A* **59**, 4559 (1999).
- [16] R. V. Jensen, H. Flores-Rueda, J. D. Wright, M. L. Keeler, and T. J. Morgan, *Phys. Rev. A* **62**, 053410 (2000).
- [17] A. Kips, W. Vassen, W. Hogervorst, and P. A. Dando, *Phys. Rev. A* **58**, 3043 (1998).
- [18] A. Kips, W. Vassen, and W. Hogervorst, *Phys. Rev. A* **59**, 2948 (1999).
- [19] M. L. Keeler *et al.*, *J. Phys. B* **37**, 809 (2004).
- [20] J. D. Wright, H. Flores-Rueda, W. Huang, and T. J. Morgan, *Phys. Rev. A* **79**, 052510 (2009).
- [21] X. J. Liu *et al.*, *J. Phys. B* **35**, 2069 (2002).
- [22] T. van der Veldt, W. Vassen, and W. Hogervorst, *Europhys. Lett.* **21**, 903 (1993).
- [23] J. Main, G. Wiebusch, K. Welge, J. Shaw, and J. B. Delos, *Phys. Rev. A* **49**, 847 (1994).
- [24] G. Raitzel, H. Held, L. Marmet, and H. Walther, *J. Phys. B* **27**, 2849 (1994).
- [25] A. Matzkin and T. S. Monteiro, *Phys. Rev. Lett.* **87**, 143002 (2001).
- [26] A. Matzkin, P. A. Dando, and T. S. Monteiro, *Phys. Rev. A* **66**, 013410 (2002).
- [27] B. E. Granger and C. H. Greene, *Phys. Rev. A* **62**, 012511 (2000).
- [28] R. Kachru and H. Helm, *Phys. Rev. Lett.* **55**, 1575 (1985).
- [29] R. Blümel and W. P. Reinhardt, *Chaos in Atomic Physics* (Cambridge University Press, Cambridge, England, 1997).
- [30] Some success has been achieved in developing a semiclassical framework to account for the experimental spectrum of NO in a magnetic field in terms of inelastic diffractive orbits. See A. Matzkin, M. Raouf, and D. Gauyacq, *Phys. Rev. A* **68**, 061401(R) (2003).
- [31] We have obtained data for several other scaled energies and show only two spectra here to illustrate the conclusions presented. We plan to publish an extensive experimental map with more detailed analysis covering a wide range of energies.
- [32] J. Main and G. Wunner, *Phys. Rev. A* **55**, 1743 (1997).

- [33] A. S. Bhullar, R. Blümel, and P. M. Koch, *Phys. Rev. E* **73**, 016211 (2006).
- [34] M. Courtney, N. Spellmeyer, H. Jiao, and D. Kleppner, *Phys. Rev. A* **51**, 3604 (1995).
- [35] We are aware of two MCOT calculations for molecular hydrogen for different conditions than the present experiment. See references [25,26] and D. Wang and S. Ding, *Phys. Rev. A* **71**, 013420 (2005).
- [36] There is one level in the measured spectrum from the  $R = 5$  rotational series with  $n = 9$  which may introduce small spurious effects in the recurrence spectrum.